Electrochimica Acta 97 (2013) 326–332

Contents lists available at SciVerse ScienceDirect

Electrochimica Acta

journal homepage: www.elsevier.com/locate/electacta

Oxidation of formic acid at polycarbazole-supported Pt nanoparticles

Reza B. Moghaddam, Peter G. Pickup*

Department of Chemistry, Memorial University, St. John's, Newfoundland and Labrador, Canada A1B 3X7

ARTICLE INFO

Article history:
Received 24 January 2013
Received in revised form 26 February 2013
Accepted 27 February 2013
Available online 7 March 2013

Keywords:
Formic acid
Electrocatalysis
Polycarbazole
Platinum
Impedance

ABSTRACT

Formic acid (FA) oxidation has been investigated at Pt nanoparticles (Pt NP) supported on unmodified and polycarbazole (PCZ)-modified glassy carbon (GC) electrodes in sulfuric acid solution. Cyclic voltammetry, scanning electron microscopy, and impedance spectroscopy were used to characterize the PCZ films, whereby similar electrochemical properties and somewhat different morphologies were obtained for GC/PCZ electrodes prepared with various deposition times. These films were drop coated with preformed Pt NP. It was found that while the indirect oxidation of FA was dominant at Pt NP deposited directly on GC, the presence of a PCZ film of ~10 nm thickness caused the reaction to proceed predominantly via direct oxidation. Consequently, currents for formic acid oxidation at the low potentials relevant to direct formic acid fuel cell operation were much higher. For example at 0 V vs. SCE, the current was 29 times higher at a GC/PCZ/Pt electrode than at GC/Pt. Furthermore, by varying the thickness of the PCZ layer it was shown that the resistance of the PCZ severely impedes formic acid oxidation when the Pt NP are not in close proximity to the GC surface.

1. Introduction

Offering appreciable power densities and other important properties such as negligible fuel flammability, direct formic acid fuel cells (DFAFCs) have received much attention in both industry and academia, where efforts have been increasingly made to improve their performance and efficiency [1–3]. One of the main factors that limits DFAFC performance is the formation of poisoning species (essentially adsorbed CO; CO_{ads}) during the oxidation of formic acid at the anode, which is generally based on Pd or Pt [2]. Pd is the most active metal for FA oxidation [4,5] due to prevalence of a direct oxidation pathway (*i.e.* dehydrogenation at low potentials), although slow deactivation leads to constantly decreasing DFAFC performance [2,6–8]. This drawback is ascribed to slow formation of the CO_{ads}, which can be formed as the reaction partially goes through an indirect oxidation pathway (*i.e.* dehydration followed by CO oxidation at higher potentials) [9]. Therefore, other catalysts have been also considered, among which Pt-based catalysts show lower activity than Pd but with more stable performance in FA oxidation. For pure Pt, indirect oxidation is the prevailing pathway, and so the CO_{ads} coverage quickly reaches a steady-state.

The activity of Pt for formic acid oxidation has been increased by various means, including alloying, surface modification, and the use of conducting polymer (CP) supports [10–20]. However, it has been a long standing challenge to clearly account for such promoting effects. In particular, N-containing conducting polymers such as polyaniline (PAni) [21], polypyrrole (PPy) [22], and polycarbazole (PCZ) [23] have been shown to activate the direct oxidation at Pt, but none of the reports have provided clear explanations of these effects.

In order to develop more active Pt-CP composites for FA oxidation, it is important to understand whether the CP plays a mechanistic role in the reaction (e.g. via a ligand effect or chemical interaction with formic acid or intermediates such as CO), acts as a third-body to improve geometric properties, or merely provides a high area substrate with significant electronic and ionic conductivities. To this end we have adopted a simple method for support-effect screening [24–26] based on drop coating of preformed metal catalysts onto thin layers of various electrode modifiers. This methodology has been validated by demonstration of a bifunctional mechanism for enhancement of methanol oxidation at Ru oxide supported Pt nanoparticles [24], unambiguous promotional effects of polyaniline films for FA oxidation at Pd [25], and a mechanistic effect of Ru oxide on Pt in ethanol oxidation in contrast to a ligand effect for Sn oxide [26].

In 2011, Zhou et al. [23] reported on the enhancement of FA oxidation at Pt and PtRu catalysts supported on polycarbazole. In that work, the metal particles were deposited electrochemically, resulting in uncertainties and likely variations in the metal loadings and particle sizes. Poly(*N*-vinyl carbazole)]-supported Pt has also been used for methanol electro-oxidation under alkaline conditions [27].

Herein we report on the effects of polycarbazole (PCZ) on FA oxidation at preformed Pt nanoparticles, where the remarkable

* Corresponding author. Tel.: +1 709 864 8657; fax: +1 709 864 3702.
E-mail address: ppickup@mun.ca (P.G. Pickup).

0013-4686/$ – see front matter © 2013 Elsevier Ltd. All rights reserved.
http://dx.doi.org/10.1016/j.electacta.2013.02.133

prevalence of the direct oxidation pathway reported by Zhou et al. [23] is further documented and quantified with a well controlled Pt particle size and loading. As well, we provide preliminary but important insights into the mechanism of FA oxidation at PCZ/Pt composites.

2. Experimental

2.1. Chemicals

Sulfuric acid (Fisher Scientific), formic acid (Sigma Aldrich; 98–100%), dichloromethane (Sigma Aldrich; ACS reagent, 99.9%), tetrabutylammonium hexafluorophosphate (Fluka; electrochemical grade, 99.0%), $H_2PtCl_6{\cdot}6H_2O$ (Alfa Aesar), carbazole (Alfa Aesar; 95%), sodium citrate (Anachemia), and sodium borohydride (Sigma Aldrich) were used as received. All measurements were recorded at ambient temperature under a nitrogen atmosphere following purging for 15 min.

2.2. Preparation of Pt nanoparticles

$NaBH_4$(aq) (1.5 mL; 120 mM) was added dropwise to a stirred solution of 10 mL of 3 mM H_2PtCl_6(aq) mixed with 0.6 mL of 50 mM aqueous sodium citrate [28]. Following stirring for a further 2 h, the resulting gray colloidal Pt nanoparticle solution was stored in a fridge. X-ray diffraction (XRD) measurements indicated that the average particle diameter was 5.0 ± 0.4 nm. Transmission electron microscopy (TEM) images shown in a previous report [26] confirmed the particle size obtained by XRD.

2.3. Working electrode preparation

Glassy carbon electrodes (GC; CH Instruments; 0.071 cm^2) were polished with 0.05 μm alumina and rinsed well with water before use. Polycarbazole films were galvanostatically (0.28 mA cm^{-2}) deposited from dichloromethane (DCM) containing 0.1 M tetrabutylammonium hexafluorophosphate (Bu_4NPF_6) and 0.01 M carbazole using polymerization charge densities of 9.8, 14.1, 21.1, and 28.2 mC cm^{-2} to yield GC/PCZ1, GC/PCZ2, GC/PCZ3, and GC/PCZ4, respectively. Then, a GC and the four GC/PCZ electrodes were drop coated with 8.4 μg cm^{-2} Pt NP, designated as GC/Pt and GC/PCZ/Pt, respectively.

The mass of each PCZ film can be estimated using Eq. (1) [23,29].

$$m_{PCZ} = Q_{pol} M_{PCZ} / nF \quad (1)$$

where Q_{pol}, M_{PCZ}, F, and n are the polymerization charge, molecular mass of carbazole (167.2 g mol^{-1}), Faraday constant (96485 C mol^{-1}), and calculated number of electrons associated with polymerization of one monomer (2.17 [29]), respectively. The calculated masses were 95, 136, 204, and 271 ng, for GC/PCZ1, GC/PCZ2, GC/PCZ3, and GC/PCZ4, respectively. The corresponding film thicknesses are 9.2, 15, 22, and 30 nm, based on a density of ca. 1.3 g cm^{-3}.

2.4. Instrumentation

An EG&G Model 273A Potentiostat/Galvanostat run by a PC through M270 commercial software was used for voltammetric measurements. For impedance measurements an EG&G Model 5210 Lock-in Amplifier was also used and the system was run through Power-Suite commercial software. Electrochemical impedance measurements were performed over the range of 10 kHz to 0.1 Hz using an ac amplitude of 10 mV. Before any impedance measurement, the electrode was held for 2 min at the dc offset potential to reach electrochemical equilibrium. A saturated calomel electrode (SCE) and a platinum wire formed the reference and counter electrode, respectively. For chronoamperometry, several cyclic voltammetry scans between −0.25 and +0.8 V were run on a freshly prepared electrode in 0.1 M H_2SO_4 and then FA was injected into the cell at open circuit. Following purging again with N_2, the potential was stepped from the open circuit potential to −0.2 V, and then progressively in 100 mV steps to +0.8 V.

A Model FEI Quanta 400 environmental SEM was used to perform scanning electron microscopy (SEM) measurements.

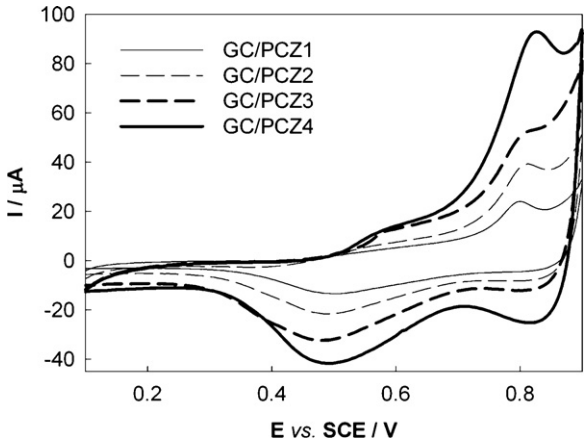

Fig. 1. Cyclic voltammograms at 100 mV s^{-1} of GC/PCZ electrodes in 0.1 M H_2SO_4.

3. Results

3.1. Characterization of the GC/PCZ electrodes

In a previous study of the effects of PCZ on FA oxidation [23], the PCZ films were deposited on GC electrodes from boron trifluoride diethylether (BFEE) containing 20% diethylether. Here we employed dichloromethane as the solvent for PCZ deposition in order to avoid the hazards of BFEE and obtain better reproducibility.

Fig. 1 shows cyclic voltammograms of the GC/PCZ electrodes in 0.1 M H_2SO_4. Forward scans (*i.e.* anodic) show onsets for oxidation of the PCZ at ca. +0.45 V and a single dominate oxidation peak at +0.82 V. These anodic features are assigned to an oxidative transition (p-doping) of the insulating neutral PCZ films to conductive states [23,30,31]. On the reverse scans, the electrodes showed two reductions centered at ca. +0.82 and +0.48 V, the former of which was less pronounced for the thinner films. These voltammograms are very similar to those reported for PCZ deposited from BFEE [23].

Scanning electron micrographs (SEM) are shown in Fig. 2 for further characterization of the GC/PCZ films. GC/PCZ1 and GC/PCZ2 show leaf-like structures similar to those reported for PCZ deposited from BFEE [23], while rod-like structures are observed for the thicker GC/PCZ3 and GC/PCZ4 films.

3.2. Formic acid oxidation: cyclic voltammetry

Fig. 3 shows cyclic voltammograms of a GC/Pt electrode in 0.1 M H_2SO_4 (A), and in the presence of 0.5 M FA (B). The blank voltammogram (A) displays characteristic signals of pure Pt in an acid medium [32], where hydrogen electrochemistry can be seen below $E \sim 0$ V with H desorption on the forward (*i.e.* anodic) scan and H adsorption on the reverse scan, as indicated in the figure. Also, well defined oxide formation/stripping peaks can be seen at higher potentials, where the oxide formation wave begins at ∼+0.4 V on the forward scan and there is an oxide stripping peak at ∼+0.35 V on the reverse scan. By integrating the area under the peaks, one can estimate charge densities for H adsorption and desorption. Considering